

## Dark States and Interferences in Cascade Transitions of Ultra-Cold Atoms in a Cavity

R. Arun and G. S. Agarwal

Physical Research Laboratory, Navrangpura, Ahmedabad 380 009, India

(February 2, 2022)

We examine the competition among one- and two-photon processes in an ultra-cold, three-level atom undergoing cascade transitions as a result of its interaction with a bimodal cavity. We show parameter domains where two-photon transitions are dominant and also study the effect of two-photon emission on the maser action in the cavity. The two-photon emission leads to the loss of detailed balance and therefore we obtain the photon statistics of the cavity field by the numerical integration of the master equation. The photon distribution in each cavity mode exhibits sub- and super-Poissonian behaviors depending on the strength of atom-field coupling. The photon distribution becomes identical to a Poisson distribution when the atom-field coupling strengths of the modes are equal.

PACS number(s): 42.50.Vk, 42.50.Dv, 03.75.-b

## I. INTRODUCTION

The dynamics of atom-field coupling in high quality cavities has been an interesting tool to verify the predictions of quantum electrodynamics (QED) on the radiation-matter interaction [1,5]. The properties of atoms in cavities can be modified in a controlled way by the proper design of cavity geometry and its quality factors. For example, the spontaneous emission of an atom can be enhanced or inhibited inside a cavity [3]. Cavities with high quality factors are especially attractive for studying the regime of strong interaction between the atoms and the quantized fields. Interesting effects of strong interaction such as collapse and revival of Rabi oscillations, vacuum Rabi splitting, atom-atom and atom-field entanglements have been predicted and observed [4,5]. The generation of atom-field entangled states in cavity QED finds many applications in quantum information processing, logic gates etc. A very important result of strong interaction was the micromaser where the excited atoms go successively through a high quality cavity in a time much smaller than the characteristic decay times. This leads to build up of a steady state field in the cavity which has properties quite different from laser fields. The theoretical works on micromaser [6,7] suggested the sub-Poissonian photon statistics which is purely due to the quantum nature of the field. The operation of the micromaser has been realized [8] and Weidinger et al verified the existence of trapping states in the micromaser [9]. The two-photon micromaser as well as the microlaser were also realized [10,11]. The theory of two-mode micromaser operating on three-level systems has been developed [12].

In all these works, the external motion of the atom is treated classically while its interaction with the field is quantum mechanical. By considering ultra-cold atoms, Scully et al [13] discovered that the quantum treatment of center-of-mass (c.m.) motion of an atom leads to a completely new kind of induced emission in a cavity. The dressed state analysis shows that the cavity field can act like a quantum mechanical potential for an ultra-cold, incident atom. The nature of the potentials depends on the mode profile of the cavity as well as the atom-field coupling strengths [14,15]. Thus the atom besides changing its electronic states can be either reflected or transmitted through the cavity. This reflection or transmission of the atoms is very similar to those of a particle interacting with potential barriers or wells. We have recently shown that tunneling of an ultra-cold, two-level atom in the excited state through two successive cavities exhibits transmission resonances similar to those of an electron tunneling through semiconductor double barriers [16]. The reflection and transmission through cavity induced potentials give rise to many interesting features in the photon statistics and the spectrum of the micromaser pumped by ultra-cold atoms [17]. Further, the works on quantum treatment of the atomic motion have been extended to study the interaction of two- and three-level atoms with a single mode field [18]. Considering the quantized motion of  $\Lambda$ -type three-level atoms, the photon statistics of a two-mode micromaser was discussed [19]. In the  $\Lambda$ -type scheme, an excited atom can make only one photon transition to either of the two ground levels. In this paper, we examine the photon statistics of a two-mode micromaser pumped by ultra-cold, cascade three-level atoms. The excited atom in the cascade transition emits photons sequentially in each of the two cavity modes. Thus, the field mode which is resonant with the upper transition of the  $\Lambda$ -type atoms, gets populated by both one and two-photon transitions from the excited state. We discuss the effect of two-photon emissions from the excited atoms on the photon statistics of the micromaser. We make use of methods similar to those in Ref. [17].

The organization of the paper is as follows. In Sec. II, we describe the interaction of ultra-cold,  $\Lambda$ -type three-level atoms with the bimodal field in the cavity. We show that the field can always induce two-photon transition in an excited atom when the corresponding one-photon transition is forbidden. In Sec. III, we study the master equation and derive the master equation for the reduced density operator of the field in the cavity. In Sec. IV, the numerical results are presented for the steady state photon distribution in each mode of the bimodal field. We find that the photon distribution in each mode exhibits Poissonian statistics if the atom-field coupling strengths of the cavity modes are equal and when the two-photon transitions from the excited atoms are dominant. For different coupling strengths of the cavity modes, the dominant two-photon effects in transitions can also lead to sub- and super-Poissonian statistics of photons in the steady state field. Finally, we consider the master equation when the pumping atoms have kinetic energies close to the vacuum coupling energy. In this case, one-photon effects also become important and these lead to different photon statistics for the two cavity modes.

## II. ONE AND TWO PHOTON PROCESSES IN ULTRACOLD ATOMS IN A CAVITY

We consider a bimodal cavity of length  $L$  pumped steadily by a beam of ultra-cold three-level atoms in the cascade configuration. The scheme of our model is shown in Fig. 1. The transitions  $a \rightarrow b_1$  and  $b_1 \rightarrow b_2$  are dipole allowed while the direct transition  $a \rightarrow b_2$  is dipole forbidden. Thus the atom in the excited level  $a$  can reach the ground level  $b_2$  only through the two-photon transition  $a \rightarrow b_1 \rightarrow b_2$ . The frequencies of the two cavity modes 1 and 2 are tuned

to those of atomic transitions  $a \rightarrow b_1$  and  $b_1 \rightarrow b_2$  respectively. The Hamiltonian describing this resonant atom - eld interaction including the quantized motion of center-of-mass of the atoms along the  $z$  direction is given by

$$H = H_A + H_F + H_{AF}; \quad (1)$$

where  $H_A$  ( $H_F$ ) is the Hamiltonian of the free atom (eld) and  $H_{AF}$  is the interaction Hamiltonian describing the atom - eld interaction in the dipole and the rotating wave approximations:

$$H_A = \frac{p_z^2}{2m} + \hbar \sum_{j=1}^2 \omega_j a_j^\dagger a_j + \hbar \sum_{j=1}^2 \omega_j b_j^\dagger b_j;$$

$$H_F = \hbar \sum_{\nu=1}^2 \omega_\nu a_\nu^\dagger a_\nu;$$

$$H_{AF} = \hbar g_1 (a_1^\dagger a_1 b_1^\dagger b_1 + a_1^\dagger a_1 b_1^\dagger b_1) + \hbar g_2 (a_2^\dagger a_2 b_2^\dagger b_2 + a_2^\dagger a_2 b_2^\dagger b_2): \quad (2)$$

The operator  $a_j^\dagger a_j$  ( $j = a; b_1; b_2$ ) gives the projection on to the state  $|j\rangle$  with energy  $\hbar \omega_j$ . The operators  $a_j^\dagger a_j$  and  $b_j^\dagger b_j$  describe the atomic transitions from the upper and lower levels to the middle level. The operators  $a_\nu^\dagger$  ( $a_\nu$ ) annihilate (create) a photon in the modes  $\nu = 1; 2$  with resonance frequencies  $\omega_1 = \omega_a - \omega_{b_1}$  and  $\omega_2 = \omega_{b_1} - \omega_{b_2}$  respectively. The first and second terms in the interaction operator  $H_{AF}$  represents the action of elds 1 and 2 of the cavity on the upper ( $a, b_1$ ) and the lower ( $b_1, b_2$ ) transitions respectively. The parameters  $g$  are the corresponding atom - eld coupling constants and  $m$  is the atomic mass. The parameters  $g$  are dependent on  $z$  through the mode function of the cavity.

In the interaction picture, the Hamiltonian (1) of the atom - eld system reads

$$H_I = \frac{p_z^2}{2m} + H_{AF}; \quad (3)$$

It is useful to expand the interaction Hamiltonian  $H_{AF}$  in its diagonal basis. The operator  $H_{AF}$  has eigenstates  $|j_{n_1+1; n_2+1}^0\rangle, |j_{n_1+1; n_2+1}\rangle$  with eigenvalues 0;  $\hbar \frac{g_1^2(z)(n_1+1) + g_2^2(z)(n_2+1)}{2}$ , respectively, where

$$\begin{aligned} |j_{n_1+1; n_2+1}^0\rangle &= \frac{g_2^{n_2+1}}{g_1^{n_1+1} + g_2^{n_2+1}} |a; n_1; n_2\rangle - \frac{g_1^{n_1+1}}{g_1^{n_1+1} + g_2^{n_2+1}} |b_2; n_1+1; n_2+1\rangle \\ |j_{n_1+1; n_2+1}\rangle &= \frac{1}{2} \left[ \frac{g_1^{n_1+1}}{g_1^{n_1+1} + g_2^{n_2+1}} |a; n_1; n_2\rangle + |b_1; n_1+1; n_2\rangle \right. \\ &\quad \left. + \frac{g_2^{n_2+1}}{g_1^{n_1+1} + g_2^{n_2+1}} |b_2; n_1+1; n_2+1\rangle \right] \end{aligned} \quad (4)$$

The interaction operator  $H_{AF}$  and its eigenstates  $|j_{n_1+1; n_2+1}^0\rangle, |j_{n_1+1; n_2+1}\rangle$  depend on the position  $z$  through the coupling strengths  $g_1(z), g_2(z)$ . Thus, it is in general difficult to carry out the time evolution of an atom - eld state governed by the Hamiltonian (3) for the quantized motion of atoms. So, for simplicity, we work with the meso mode functions  $g(z) = g_0(z) (L - z)$  which represent the constant eld modes in the cavity. In this case, the eigenstates of the interaction are independent of atomic position inside the cavity and the atomic motion sees free particle evolution in the dark state of interaction  $|j_{n_1+1; n_2+1}^0\rangle$ . The effect of atom's interaction with the cavity on its external motion can be realized only in the dressed state  $|j_{n_1+1; n_2+1}\rangle$  components of the initial atom - eld state. We need to consider the initial atom - eld state to be  $|a; n_1; n_2\rangle$ , i.e., the atom is in the excited state and the cavity contains  $(n_1; n_2)$  photons in the modes (1;2) initially. This initial state can be expanded in the dressed state basis as

$$\begin{aligned} |a; n_1; n_2\rangle &= \frac{g_1^{n_1+1}}{g_1^{n_1+1} + g_2^{n_2+1}} |j_{n_1+1; n_2+1}^+\rangle + |j_{n_1+1; n_2+1}^0\rangle \\ &\quad + \frac{g_2^{n_2+1}}{g_1^{n_1+1} + g_2^{n_2+1}} |j_{n_1+1; n_2+1}^-\rangle; \end{aligned} \quad (5)$$

The time evolution of this initial state can be found by expanding the combined state of atom-cavity system as

$$|j(z;t)\rangle = |n_1+1, n_2+1\rangle \langle j| + |n_1+1, n_2+1\rangle \langle j| + |0\rangle \langle j|_{n_1+1, n_2+1} \quad (6)$$

then the time dependent Schrodinger equation becomes

$$i\hbar \frac{\partial}{\partial t} |j(z;t)\rangle = H |j(z;t)\rangle; \quad |j(z;0)\rangle = |j\rangle; \quad (7)$$

Here,  $H = p_z^2/2m + \hbar \frac{p}{g_1^2(n_1+1) + g_2^2(n_2+1)}$ ,  $H_0 = p_z^2/2m$  are operators acting in the space of center of mass variables. Thus, the effect of the cavity with fixed number of photons produces potential terms in  $H$  corresponding to the dressed states  $|j\rangle_{n_1+1, n_2+1}$  as discussed in Ref. [17]. The barrier and well potentials induced by the interaction for the atomic motion in the states  $|j\rangle_{n_1+1, n_2+1}$  are then displayed as in Fig. 2. It is also important to note that the external motion of atom experiences free time evolution in the dark state  $|j\rangle_{n_1+1, n_2+1}^0$  for the mesamode distribution of the cavity fields. Denoting the reflection and transmission amplitudes as  $r_{n_1, n_2}$ ,  $t_{n_1, n_2}$  for the potential barrier-well problem of the dressed states  $|j\rangle_{n_1+1, n_2+1}$ , respectively, we have

$$|j\rangle_{n_1, n_2} = |j\rangle_{n_1, n_2} \sin(k_{n_1, n_2} L) \exp(ikL) |j\rangle_{n_1, n_2}; \quad (8)$$

$$|j\rangle_{n_1, n_2} = \exp(-ikL) \cos(k_{n_1, n_2} L) |j\rangle_{n_1, n_2} \sin(k_{n_1, n_2} L)^{-1}; \quad (9)$$

$$r_{n_1, n_2} = \frac{1}{2} \frac{k_{n_1, n_2}}{k} - \frac{k}{k_{n_1, n_2}}; \quad (10)$$

$$t_{n_1, n_2} = \frac{1}{2} \frac{k_{n_1, n_2}}{k} + \frac{k}{k_{n_1, n_2}}; \quad (11)$$

$$k_{n_1, n_2} = \frac{1}{2} \frac{2m}{\hbar} \frac{g_1^2(n_1+1) + g_2^2(n_2+1)}{k}; \quad (12)$$

where  $\hbar k$  is the atomic momentum and  $L$  is the length of the cavity. It is to be noted that the strengths of the barrier-well potentials (potential energy term in  $k_{n_1, n_2}$ ) depend on the coupling constants  $g_1, g_2$  as well as the occupation numbers  $n_1, n_2$  of the photons in the cavity.

We consider the initial wave packet of the moving free atom to be  $|\psi(z;t)\rangle = \exp(-ip_z^2 t/2m\hbar) \int dk A(k) e^{ikz} = \int dk A(k) e^{i(\hbar k^2/2m)t} e^{ikz}$ . The Fourier amplitudes  $A(k)$  are adjusted such that the peak of the incident wave packet  $|\psi(0;t)\rangle$  at the entry ( $z=0$ ) of the cavity occurs at time  $t=0$ . The combined state of the atom-cavity system at the initial time  $t=0$  is therefore,

$$|j(z;0)\rangle = |j\rangle_{n_1, n_2} \langle j|; \quad (13)$$

The wave function of the atom-field system at time  $t$  is found by solving the Eqs. (6) and (7) subject to the above initial condition:

$$|j(z;t)\rangle = \int dk A(k) e^{i(\hbar k^2/2m)t} [R_{a, n_1, n_2}(k) e^{ikz} (z) + T_{a, n_1, n_2}(k) e^{ikz} (z-L)] |j\rangle_{n_1, n_2} \\ + [R_{b, n_1+1, n_2}(k) e^{ikz} (z) + T_{b, n_1+1, n_2}(k) e^{ikz} (z-L)] |j\rangle_{n_1+1, n_2} \\ + [R_{b, n_1+1, n_2+1}(k) e^{ikz} (z) + T_{b, n_1+1, n_2+1}(k) e^{ikz} (z-L)] |j\rangle_{n_1+1, n_2+1}; \quad (14)$$

where

$$R_{a, n_1, n_2} = \frac{g_1^2(n_1+1)}{2(g_1^2(n_1+1) + g_2^2(n_2+1))} + \frac{1}{n_1, n_2} + \frac{1}{n_1, n_2}; \quad (15)$$

$$T_{a, n_1, n_2} = \frac{g_1^2(n_1+1)}{2(g_1^2(n_1+1) + g_2^2(n_2+1))} + \frac{1}{n_1, n_2} + \frac{1}{n_1, n_2} + \frac{g_2^2(n_2+1)}{(g_1^2(n_1+1) + g_2^2(n_2+1))}; \quad (16)$$

are the reflection and transmission amplitudes for the excited state of the atom with the initial  $(n_1; n_2)$  photons remaining in the two cavity modes and

$$\begin{aligned} R_{b_1, n_1+1; n_2} &= \frac{P}{2} \frac{g_1^2 (n_1+1)}{(g_1^2 (n_1+1) + g_2^2 (n_2+1))} + \frac{P}{2} \frac{g_1^2 (n_1+1)}{(g_1^2 (n_1+1) + g_2^2 (n_2+1))} + \frac{P}{2} \frac{g_1^2 (n_1+1)}{(g_1^2 (n_1+1) + g_2^2 (n_2+1))} ; \\ T_{b_1, n_1+1; n_2} &= \frac{P}{2} \frac{g_1^2 (n_1+1)}{(g_1^2 (n_1+1) + g_2^2 (n_2+1))} + \frac{P}{2} \frac{g_1^2 (n_1+1)}{(g_1^2 (n_1+1) + g_2^2 (n_2+1))} + \frac{P}{2} \frac{g_1^2 (n_1+1)}{(g_1^2 (n_1+1) + g_2^2 (n_2+1))} ; \end{aligned} \quad (15)$$

are the probability amplitudes that the excited atom goes to the state  $|j_1\rangle$  and emits a photon in mode 1 while getting reflected and transmitted respectively. Similarly, the excited atom is reflected or transmitted and emits a photon in both the cavity modes while making a transition to the ground state  $|j_2\rangle$  via the middle state  $|j_1\rangle$  with probability amplitudes

$$\begin{aligned} R_{b_2, n_1+1; n_2+1} &= \frac{P}{2} \frac{g_1 g_2 (n_1+1)(n_2+1)}{(g_1^2 (n_1+1) + g_2^2 (n_2+1))} + \frac{P}{2} \frac{g_1 g_2 (n_1+1)(n_2+1)}{(g_1^2 (n_1+1) + g_2^2 (n_2+1))} ; \\ T_{b_2, n_1+1; n_2+1} &= \frac{P}{2} \frac{g_1 g_2 (n_1+1)(n_2+1)}{(g_1^2 (n_1+1) + g_2^2 (n_2+1))} + \frac{P}{2} \frac{g_1 g_2 (n_1+1)(n_2+1)}{(g_1^2 (n_1+1) + g_2^2 (n_2+1))} : \end{aligned} \quad (16)$$

It is clear from the above equations that the effects of the barrier and well potentials induced by the dressed states  $|j_{n_1+1; n_2+1}\rangle$  add coherently in either the reflection or transmission of the atom. The additive term to the barrier-well amplitudes in Eqs. (14) and (16) comes from the contribution of the dark state  $|j_{n_1+1; n_2+1}^0\rangle$  in the initial state expansion Eq. (5). Since the dark state is orthogonal to the middle state  $|j_1\rangle$ , it influences only the two-photon emissions and not the one-photon emissions of the excited atom. An important feature here is that the two-photon transition can always be induced by the field when the one-photon transition is forbidden. This can be seen by examining the probabilities for different states of the atom. When an initially excited atom is incident upon the cavity containing  $(n_1; n_2)$  photons in the two cavity modes (1;2), respectively, then from Eqs. (15) and (16) the probability that the atom makes a one-photon transition to the state  $|j_1\rangle$  with the emission of a photon in mode 1 is

$$P_{n_1, n_2} (a \rightarrow b_1) = \mathcal{R}_{b_1, n_1+1; n_2}^2 + \mathcal{T}_{b_1, n_1+1; n_2}^2 ; \quad (17)$$

and the probability that the atom makes a two-photon transition to the state  $|j_2\rangle$  with the emission of a photon in each of the modes 1 and 2 of the cavity is

$$P_{n_1, n_2} (a \rightarrow b_2) = \mathcal{R}_{b_2, n_1+1; n_2+1}^2 + \mathcal{T}_{b_2, n_1+1; n_2+1}^2 : \quad (18)$$

When  $g_2 = 0$ , the lower transition  $b_1 \rightarrow b_2$  is forbidden and hence the two-photon transition probability  $P_{n_1, n_2} (a \rightarrow b_2)$  vanishes. Then, the upper transition  $a \rightarrow b_1$  behaves like a two-level atom interacting with the mode 1 of the cavity field. In Fig. 3, we compare the photon emission probabilities of excited, two-level ( $g_2 = 0$ ) and three-level ( $g_2 \neq 0$ ) atoms when the cavity is initially in vacuum state. We scale the parameters in terms of a wave number which is defined by the vacuum coupling energy  $\hbar g_1 = \hbar^2 / 2m$  of the two-level atom. Note that the coupling strength  $g_1 = 2 \times 10$  MHz of a  $^{85}\text{Rb}$  atom corresponds to 155  $\mu\text{m}$  length of the cavity for the parameter  $L = 20000$ . The temperature of the atom is of the order of  $10^{-8}$  K for the mean momentum  $k = 0.01$ . For ultra-cold, incident atoms ( $k \ll 1$ ), the graph in Fig. 3(a) shows that the one-photon emission probability exhibits resonances as a function of length of the cavity for both two-level and three-level atoms. In the three-level atom, the resonances of the one-photon emission probability occur at values of  $L$  different from those of two-level atom. The two-photon emission probability shows maxima and minima at the resonance positions of the one-photon transition. This behavior arises from the interference of the contributions coming from different dressed states in the initial state expansion Eq. (5). The transmission probability  $\mathcal{T}_{b_2, n_1+1; n_2+1}^2$  obtained from Eq. (16) has an interference term proportional to the phase of the amplitude  $\frac{P}{2} \frac{g_1 g_2 (n_1+1)(n_2+1)}{(g_1^2 (n_1+1) + g_2^2 (n_2+1))}$ . This term can be constructive or destructive which leads to the enhancement or reduction of the two-photon emission probability. From the graph, we also see that  $P_{0,0} (a \rightarrow b_2) = 0.32$  when  $P_{0,0} (a \rightarrow b_1) = 0$ . This implies that the probability of two-photon emission is not the product of the probabilities for single photon emission. This also suggests that both the field modes of the binodal cavity can be amplified together through the two-photon transition of an excited atom. This feature is absent in the case of two-mode micromaser pumped by ultra-cold,  $\Lambda$ -type three-level atoms [19]. In the  $\Lambda$ -scheme micromaser, the excited atom can make only one-photon transition to either of the two ground levels. Therefore, both the cavity modes can not be populated sequentially by the photon emission from the same atom. Next, we compare our results for ultra-cold atoms with that of fast, incident atoms in the  $\Lambda$ -type configuration. In the case of fast, incident atoms ( $k \gg 1$ ), both one-

and two-photon emission probabilities exhibit Rabi oscillations as a function of the length of the cavity as seen from Fig. 3(b). The Rabi frequency of oscillation for one-photon emission is twice that of the two-photon emission. These features resemble exactly the results in the usual Jaynes-Cummings (JC) model where one neglects the quantization of the atomic motion in atom-cavity interaction [2]. Thus, neglecting the kinetic energy operator in the Hamiltonian (1), the time evolution of the initial atom-field state  $|j; n_1; n_2\rangle$  gives for the photon emission probabilities in the JC model:

$$P_{n_1; n_2} (a \rightarrow b_1) = \frac{g_1^2 (n_1 + 1)}{2} \sin^2 \left( \frac{\Omega}{2} \right);$$

$$P_{n_1; n_2} (a \rightarrow b_2) = \frac{4g_1^2 g_2^2 (n_1 + 1) (n_2 + 1)}{4} \sin^4 \left( \frac{\Omega}{2} \right);$$

where  $\Omega = \sqrt{g_1^2 (n_1 + 1) + g_2^2 (n_2 + 1)}$  is the Rabi frequency and  $\tau$  is the interaction time of the atom with the cavity. Note that when  $\tau$  is an odd number multiple of  $\pi/\Omega$ , the one-photon transition is forbidden and the two-photon transition probability becomes maximum consistent with the results for fast atoms in Fig. 3.

### III. MAZER ACTION IN A BIMODAL CAVITY - BASIC MASTER EQUATION FOR THE CAVITY FIELD

In this section, we consider the maser action of ultracold atoms in a bimodal cavity and derive the master equation for the cavity field assuming that excited atoms are pumped steadily into the cavity. We model the random pumping of the atoms into the cavity by a Poissonian process with an average rate of pumping  $r$ . The flux of the incident atoms is adjusted so that only one atom interacts with the cavity field at a time. We neglect the cavity field damping during the time an atom interacts with the field. Since the field in the cavity changes with the passage of each atom, we need to know the time evolution of the atom-field state for a general initial state of the cavity field. The wave function of the initial atom-field system is now given by

$$|j(z; 0)\rangle = \sum_{n_1; n_2} C_{n_1; n_2} |j; n_1; n_2\rangle; \quad (19)$$

Carrying out the time evolution for this initial state using Eqs. (5)-(7), the state of atom-field system after the interaction is given by

$$\begin{aligned} |j(z; t)\rangle = & \sum_{n_1; n_2=0}^{\infty} \int dk A(k) e^{i(\hbar k^2 - 2m) t} \\ & R_{a; n_1; n_2}(k) e^{ikz} (z) |j; n_1; n_2\rangle + T_{a; n_1; n_2}(k) e^{ikz} (z-L) |j; n_1; n_2\rangle \\ & + R_{b_1; n_1+1; n_2}(k) e^{ikz} (z) |j; n_1+1; n_2\rangle + T_{b_1; n_1+1; n_2}(k) e^{ikz} (z-L) |j; n_1+1; n_2\rangle \\ & + R_{b_2; n_1+1; n_2+1}(k) e^{ikz} (z) |j; n_1+1; n_2+1\rangle + T_{b_2; n_1+1; n_2+1}(k) e^{ikz} (z-L) |j; n_1+1; n_2+1\rangle; \end{aligned} \quad (20)$$

where

$$\begin{aligned} R_{a; n_1; n_2}(k) &= C_{n_1; n_2} R_{a; n_1; n_2}(k); \\ T_{a; n_1; n_2}(k) &= C_{n_1; n_2} T_{a; n_1; n_2}(k); \end{aligned} \quad (21)$$

are the probability amplitudes for reflection (or) transmission of the atom in the upper state  $|j\rangle$  with  $(n_1; n_2)$  photons in the cavity field and similarly, the atom is reflected (or) transmitted when the atom-field state is  $|j; n_1+1; n_2\rangle$  (or)  $|j; n_1+1; n_2+1\rangle$  with amplitudes

$$\begin{aligned} R_{b_1; n_1+1; n_2}(k) &= C_{n_1; n_2} R_{b_1; n_1+1; n_2}(k); \\ T_{b_1; n_1+1; n_2}(k) &= C_{n_1; n_2} T_{b_1; n_1+1; n_2}(k); \\ R_{b_2; n_1+1; n_2+1}(k) &= C_{n_1; n_2} R_{b_2; n_1+1; n_2+1}(k); \\ T_{b_2; n_1+1; n_2+1}(k) &= C_{n_1; n_2} T_{b_2; n_1+1; n_2+1}(k); \end{aligned} \quad (22)$$

The time evolution of the reduced density operator of the field in the interaction picture is then given in the coarse graining method [7] to be

$$\dot{\rho}(t) = \mathcal{R}(\rho(t)) + \mathcal{L}(\rho(t)) ; \quad (23)$$

where  $\rho(t) = \rho(t) - \rho(0)$  is the change in the reduced density operator of the field due to the passage of a single atom in the excited state. This can be obtained by forming the atom - field density matrix using Eqs. (19) - (22) and tracing over external and internal degrees of freedom of the atom. Field damping and the effect of thermal photons are described by the Liouville operator

$$\begin{aligned} \mathcal{L} = & \frac{1}{2} C_1 (n_{b_1} + 1) (2a_1^\dagger a_1 - a_1^\dagger a_1 - a_1^\dagger a_1) \\ & + \frac{1}{2} C_1 n_{b_1} (2a_1^\dagger a_1 - a_1^\dagger a_1 - a_1^\dagger a_1) \\ & + \frac{1}{2} C_2 (n_{b_2} + 1) (2a_2^\dagger a_2 - a_2^\dagger a_2 - a_2^\dagger a_2) \\ & + \frac{1}{2} C_2 n_{b_2} (2a_2^\dagger a_2 - a_2^\dagger a_2 - a_2^\dagger a_2) : \end{aligned} \quad (24)$$

Here  $n_b$  is the number of thermal photons in mode and  $C$  is the damping rate of this mode. Using Eqs. (23) and (24) we obtain the equation governing the time evolution of density matrix elements,

$$\begin{aligned} \dot{\rho}(n_1; n_2; n_1^0; n_2^0) = & \mathcal{R}_{a; n_1, n_2} \mathcal{R}_{a; n_1^0, n_2^0}^\dagger + \mathcal{T}_{a; n_1, n_2} \mathcal{T}_{a; n_1^0, n_2^0}^\dagger - 1) \rho(n_1; n_2; n_1^0; n_2^0) \\ & + (\mathcal{R}_{b_1; n_1, n_2} \mathcal{R}_{b_1; n_1^0, n_2^0}^\dagger + \mathcal{T}_{b_1; n_1, n_2} \mathcal{T}_{b_1; n_1^0, n_2^0}^\dagger) \rho(n_1 - 1; n_2; n_1^0 - 1; n_2^0) \\ & + (\mathcal{R}_{b_2; n_1, n_2} \mathcal{R}_{b_2; n_1^0, n_2^0}^\dagger + \mathcal{T}_{b_2; n_1, n_2} \mathcal{T}_{b_2; n_1^0, n_2^0}^\dagger) \rho(n_1 - 1; n_2 - 1; n_1^0 - 1; n_2^0 - 1) \\ & + \frac{1}{2} C_1 (n_{b_1} + 1) \mathcal{P} \frac{1}{(n_1 + 1)(n_1^0 + 1)} \rho(n_1 + 1; n_2; n_1^0 + 1; n_2^0) \\ & - \frac{1}{2} C_1 n_{b_1} \mathcal{P} \frac{1}{n_1 n_1^0} \rho(n_1 - 1; n_2; n_1^0 - 1; n_2^0) \\ & + \frac{1}{2} C_2 (n_{b_2} + 1) \mathcal{P} \frac{1}{(n_2 + 1)(n_2^0 + 1)} \rho(n_1; n_2 + 1; n_1^0; n_2^0 + 1) \\ & - \frac{1}{2} C_2 n_{b_2} \mathcal{P} \frac{1}{n_2 n_2^0} \rho(n_1; n_2 - 1; n_1^0; n_2^0 - 1) \\ & + \frac{1}{2} C_2 n_{b_2} \mathcal{P} \frac{1}{n_2 n_2^0} \rho(n_1; n_2 - 1; n_1^0; n_2^0 - 1) : \end{aligned} \quad (25)$$

The diagonal elements of the density matrix  $P(n_1; n_2) = \rho(n_1; n_2; n_1; n_2)$  which gives the joint distribution of photons in the two cavity modes, obeys the following equation:

$$\begin{aligned} \dot{P}(n_1; n_2) = & G_{b_1; n_1, n_2} P(n_1; n_2) + G_{b_1; n_1 - 1, n_2} P(n_1 - 1; n_2) \\ & + G_{b_2; n_1, n_2} P(n_1; n_2) + G_{b_2; n_1, n_2 - 1} P(n_1; n_2 - 1) \\ & + C_1 (n_{b_1} + 1) [(n_1 + 1)P(n_1 + 1; n_2) - n_1 P(n_1; n_2)] \\ & + C_1 n_{b_1} [n_1 P(n_1 - 1; n_2) - (n_1 + 1)P(n_1; n_2)] \\ & + C_2 (n_{b_2} + 1) [(n_2 + 1)P(n_1; n_2 + 1) - n_2 P(n_1; n_2)] \\ & + C_2 n_{b_2} [n_2 P(n_1; n_2 - 1) - (n_2 + 1)P(n_1; n_2)] ; \end{aligned} \quad (26)$$

where  $G_{b_1; n_1, n_2} = \mathcal{R}_{b_1; n_1, n_2} P_{n_1, n_2}(a \rightarrow b_1)$  and  $G_{b_2; n_1, n_2} = \mathcal{R}_{b_2; n_1, n_2} P_{n_1, n_2}(a \rightarrow b_2)$  are the gain coefficients for the atomic transitions with  $P_{n_1, n_2}(a \rightarrow b_1)$  and  $P_{n_1, n_2}(a \rightarrow b_2)$  as defined in Eqs. (17) and (18). This is the master equation for the two-mode micromaser describing the time evolution of photon distribution in the cavity. This equation behaves similar to a rate equation for the probability and a simple physical meaning can be given to each term on the right hand side in terms of in flow and out flow of probabilities. The first and second terms in the equation gives the effect of one-photon transitions while the third and fourth terms correspond to the two-photon transitions of the excited atoms.

The steady state distribution of photons obeys the equation

$$P(n_1; n_2) = 0 \quad (27)$$

In the limit  $g_2 \rightarrow 0$ , the two-photon transition probability in Eq. (18) tends to zero and therefore we can neglect the third and fourth terms containing  $G_{b_2, n_1, n_2}$  in the master Eq. (26). In this case, the upper transitions  $a \rightarrow b_1$  behave like two-level atoms interacting with the mode 1 of the cavity. The lower transitions  $b_1 \rightarrow b_2$  and hence the two-photon transitions  $a \rightarrow b_1 \rightarrow b_2$  are forbidden in the interaction. The steady state solution of the Eq. (27) can then be obtained in analytical form by using the principle of detailed balance as discussed by Meyer et al [17]. The photon statistics in this two-level problem is a mixture of thermal and shifted thermal distributions. When  $g_2 \neq 0$ , both the one- and two-photon effects of atomic transitions contribute in building up the cavity field. The two-photon terms (third and fourth terms) in the master equation have no counterpart in the decay terms and therefore the equation is not solvable analytically for the steady state distribution by the principle of detailed balance adopted in all the previous works on micromasers. In this general case, we integrate the master equation (26) numerically using fourth order Runge kutta method to get the steady state solution. We do not use any decorrelation approximation. The photon distribution  $P_1(n)$  and  $P_2(n)$  in the cavity modes 1 and 2 are obtained respectively using

$$P_1(n) = \sum_{l=0}^n P(n; l); \quad P_2(n) = \sum_{l=0}^n P(l; n); \quad (28)$$

The normalized variances of photon distribution in the two cavity modes are defined by

$$\sigma^2 = \frac{\ln^2 i - \ln i^2}{\ln i}; \quad i = 1, 2; \quad (29)$$

In Fig. 4, we present the numerical results of the photon distribution in steady state for ultra-cold, incident atoms ( $k = \ll 1$ ) by assuming equal parameters for the decay terms  $C_1 = C_2 = C$ ,  $n_{b_1} = n_{b_2} = n_b$ . The graph shows that for  $g_1 < g_2$ , the photon statistics in mode 1 is super-Poissonian ( $\sigma_1^2 > 1$ ) while that of mode 2 is sub-Poissonian ( $\sigma_2^2 < 1$ ). The photon distribution for  $g_1 > g_2$  is identical to that of  $g_1 < g_2$  except that modes 1 and 2 are interchanged. When  $g_1 = g_2$ , each mode of the cavity field exhibits Poissonian statistics ( $\sigma^2 = 1$ ) of mean  $r = 2C - 1$ . To understand these numerical results, we now approximate the master equation (26) by dropping the first and second terms corresponding to one-photon transitions. In fact, for the parameters of Fig. 4, the barrier and well amplitudes are  $n_1, n_2 \rightarrow 0$  for wide range of  $n_1$  and  $n_2$  values. Therefore, the one-photon transition probability  $P_{n_1, n_2}(a \rightarrow b_1)$  in Eq. (17) is approximately zero. The two-photon emission probability  $P_{n_1, n_2}(a \rightarrow b_2)$  in Eq. (18) can then be approximated to be  $2g_1^2 g_2^2 (n_1 + 1)(n_2 + 1) = (g_1^2 (n_1 + 1) + g_2^2 (n_2 + 1))^2$ . Note that this approximation is also consistent with the results for ultra-cold atoms in Fig. 3. With these substitutions for the photon emission probabilities in gain coefficients, numerical integration of the master Eq. (26) again gives the same results. Moreover, in the absence of one-photon terms, the master equation is symmetric with respect to the labels 1 and 2 of the two cavity modes. Thus, the Poissonian distribution of photons in each cavity mode is purely the effect of two-photon transitions of the excited atoms. It should be emphasized that the transmission of atoms occurs only in the dark eigenstate component of the interaction during the field buildup in the cavity. The atoms interacting with the barrier-well component of the dressed states get reflected always. But both the reflected and the transmitted atoms have equal probability of two-photon emissions into the cavity. Since the one-photon emissions are forbidden in the interaction for ultracold atoms, the photon distribution of both the cavity modes peaks around the same photon number in Fig. 4. In general, the photon distribution for mode 1 peaks at a higher photon number when compared with that of mode 2. This is because the mode 1 of the cavity can be populated by both one- and two-photon emissions while the mode 2 can be populated by only two-photon emissions from the incident atoms. We have found this behavior of steady state photon distribution in the case of fast, incident atoms. In Fig. 5, we display the steady state photon distribution when the micromaser is pumped by fast, incident atoms ( $k = \gg 1$ ) for the same parameters of Fig. 4(a). The graph shows that the field 1 is amplified more than the field 2 by the stimulated, photon emissions from the incident atoms. It is important to note that the field 2 has an influence on the field 1 in the cavity through the interaction with the atoms. The effects of field 2 such as gain enhancement or gain reduction on field 1 have been already discussed in a different context viz in a two-beam laser operating on cascade three-level atoms [20]. Next, we show the effect of thermal photons in the cavity on the steady state photon distribution in Fig. 6. For comparison, we have also plotted the photon distribution for the two-level problem ( $g_2 = 0$ ). The length  $L$  of the cavity is chosen to be at a resonance of the one-photon emission probability for the initial, excited state of the two-level atom and three photons in mode

1 of the cavity. The photon distribution in the two-level problem then looks similar to a mixture of thermal and shifted thermal distributions as discussed by Meyer et al [17]. For three-level atoms, comparison with Fig. 4 (a) shows that the photon distribution broadens because of the presence of thermal photons ( $n_b \neq 0$ ) even though qualitative features are very similar. In particular, the two-photon emissions from the pumping atoms are still the dominant contribution to the steady state field for the chosen length of the cavity. The Poissonian-like statistics of photons in the micromaser cavity pumped by cold atoms, resembles closely the behavior of a laser operating at far above threshold [21]. Finally, we note that the two-photon effects are dominant over the one-photon transitions only in the limit ( $k \ll 1$ ) of ultra-slow motion of the incident atoms. The competition of the one-photon with the two-photon processes becomes stronger even for energies of the incident atoms ( $k \approx 1$ ) close to the vacuum coupling energy. In Fig. 7, we plot the photon distribution in the cavity for the mean momentum  $k = 1.1$  of the incident atoms. The inset of the Fig. 7 shows the photon emission probabilities of an excited atom for an initial, vacuum state of the cavity field. The graph shows that the one-photon effects participate in the field build up of the cavity and these lead to unequal, average number of photons in the two modes of the maser field.

## V. SUMMARY

We considered the interaction of mono-energetic beam of ultra-cold, cascade three-level atoms in the excited state with a bimodal cavity. The atom-field interaction is equivalent to reflection and transmission of the atoms through the potentials induced by the dressed states. There is also a reflection-less transmission of the atoms in the dark eigenstate of atom-field interaction. We find that two-photon transition can always be induced in an excited atom when its one-photon transition is forbidden. In general, the two-photon emissions from the excited atoms dominate over the one-photon emissions in building up the steady state field of the cavity. The steady state photon distribution in each mode exhibits sub- and super-Poissonian behaviors depending on the strengths of the atom-field couplings. The photon distribution approaches the Poissonian statistics when the atom-field coupling strengths of the two modes are equal. We have also obtained the photon distribution in steady state when the micromaser is pumped by fast, moving atoms instead of ultracold atoms. In this case, both one- and two-photon emissions from the incident atoms contribute in building up the steady field of the cavity.

- 
- [1] See the articles by G. Raithel, C. W. Wagner, H. Walther, L. M. Narducci and M. O. Scully, in *Cavity Quantum Electrodynamics*, edited by P. R. Bernan (Academic, Boston, 1994), p. 57; S. Haroche and J. M. Raimond, *ibid.* p. 123; H. J. Kimble, *ibid.* p. 203.
  - [2] H. -I. Yoo and J. H. Eberly, *Phys. Rep.* 118, 239 (1985).
  - [3] P. Goy, J. M. Raimond, M. Gross, and S. Haroche, *Phys. Rev. Lett.* 50, 1903 (1983); D. Kleppner, *ibid.* 47, 233 (1981).
  - [4] J. H. Eberly, N. B. Narozhny, and J. J. Sanchez-Mondragon, *Phys. Rev. Lett.* 44, 1323 (1980); J. J. Sanchez-Mondragon, N. B. Narozhny, and J. H. Eberly, *ibid.* 51, 550 (1983); G. S. Agarwal, *ibid.* 53, 1732 (1984); F. Bernardot, P. Nussenzweig, M. Brune, J. M. Raimond, and S. Haroche, *Europhys. Lett.* 17, 33 (1992).
  - [5] J. M. Raimond, M. Brune, and S. Haroche, *Rev. Mod. Phys.* 73, 565 (2001).
  - [6] P. Filipowicz, J. Javanainen, and P. Meystre, *Phys. Rev. A* 34, 3077 (1986).
  - [7] L. A. Lugiato, M. O. Scully, and H. Walther, *Phys. Rev. A* 36, 740 (1987).
  - [8] D. Meschede, H. Walther, and G. Muller, *Phys. Rev. Lett.* 54, 551 (1985); G. Rempe, F. Schmidt-Kaler, and H. Walther, *ibid.* 64, 2783 (1990).
  - [9] M. Weidinger, B. T. H. Varcoe, R. Heerlein, and H. Walther, *Phys. Rev. Lett.* 82, 3795 (1999).
  - [10] M. Brune, J. M. Raimond, P. Goy, L. Davidovich, and S. Haroche, *Phys. Rev. Lett.* 59, 1899 (1987).
  - [11] K. An, J. J. Childs, R. R. Dasari, and M. S. Feld, *Phys. Rev. Lett.* 73, 3375 (1994).
  - [12] Fam Le Kien, G. M. Meyer, M. O. Scully, H. Walther, and Shi-Yao Zhu, *Phys. Rev. A* 49, 1367 (1994).
  - [13] B. -G. Englert, J. Schwinger, A. O. Banut, and M. O. Scully, *Europhys. Lett.* 14, 25 (1991); M. O. Scully, G. M. Meyer and H. Walther, *Phys. Rev. Lett.* 76, 4144 (1996).
  - [14] Note that [C. J. Hood, M. S. Chapman, T. W. Lynn, and H. J. Kimble, *Phys. Rev. Lett.* 80, 4157 (1998); P. M. Unsternann, T. Fischer, P. M. Aunz, P. W. H. Pinkse, and G. Rempe, *Phys. Rev. Lett.* 82, 3791 (1999)] have already reported mechanical forces on atoms in a cavity with less than one photon on the average.
  - [15] [J. C. Retamal, E. Solano and N. Zagury, *Opt. Commun.* 154, 28 (1998)] discuss the effects of periodic potentials in the interaction of an ultra-cold, two-level atom with a sinusoidal mode field.
  - [16] G. S. Agarwal and R. A. Run, *Phys. Rev. Lett.* 84, 5098 (2000).
  - [17] G. M. Meyer, M. O. Scully, and H. Walther, *Phys. Rev. A* 56, 4142 (1997); M. Loefer, G. M. Meyer, M. Schroder, M. O. Scully, and H. Walther, *ibid.* 56, 4153 (1997); M. Schroder, K. Vogel, W. P. Schleich, M. O. Scully, and H. Walther, *ibid.* 56, 4164 (1997).
  - [18] Z.-M. Zhang and L.-S. He, *Chin. Phys. Lett.* 16, 26 (1999); Z.-M. Zhang, S.-W. Xie, Y.-L. Chen, Y.-X. Xia and S.-K. Zhou, *Phys. Rev. A* 60, 3321 (1999); Z.-M. Zhang, Z.-Y. Lu and L.-S. He, *Phys. Rev. A* 59, 808 (1999).
  - [19] R. A. Run, G. S. Agarwal, M. O. Scully, and H. Walther, *Phys. Rev. A* 62, 023809 (2000).
  - [20] Shi-Yao Zhu and M. O. Scully, *Phys. Rev. A* 38, 5433 (1988).
  - [21] M. O. Scully and M. S. Zubairy, *Quantum Optics*, Cambridge University Press 1997.

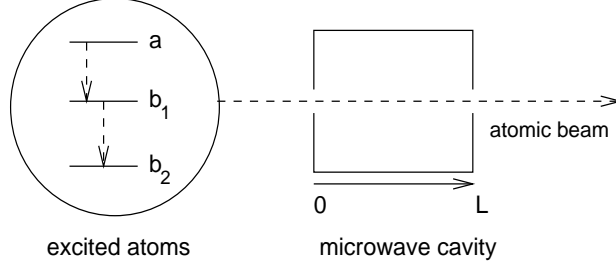


FIG . 1. The scheme of the two-mode microwave cavity pumped by  $\Lambda$ -type three-level atoms in the excited state.

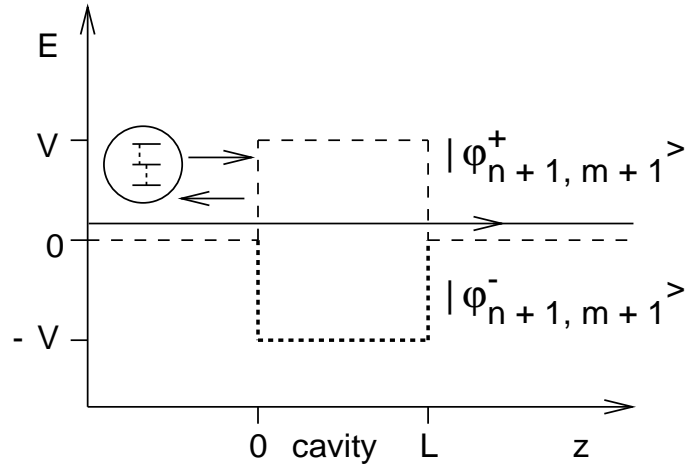


FIG . 2. Schematic representation of the energy  $E$  of the excited atoms incident upon a two-mode microwave cavity with  $(n; m)$  photons. The atom-field interaction creates a barrier (dashed) and well (dotted) potentials with a potential energy  $V = \hbar \sqrt{g_1^2(n+1) + g_2^2(m+1)}$  in the dressed states  $j_{n+1, m+1}^i$ . The scattering from these cavity induced potentials leads to reflection or transmission of the atoms through the cavity. The interaction also induces a reflection-less transmission of the atoms in the dark state  $j_{n+1, m+1}^0$ . However, the reflection or transmission of the atoms can occur only in either of the three states  $j_{n; m}^i$ ,  $j_{n+1; m}^i$ , and  $j_{n+1; m+1}^i$ .

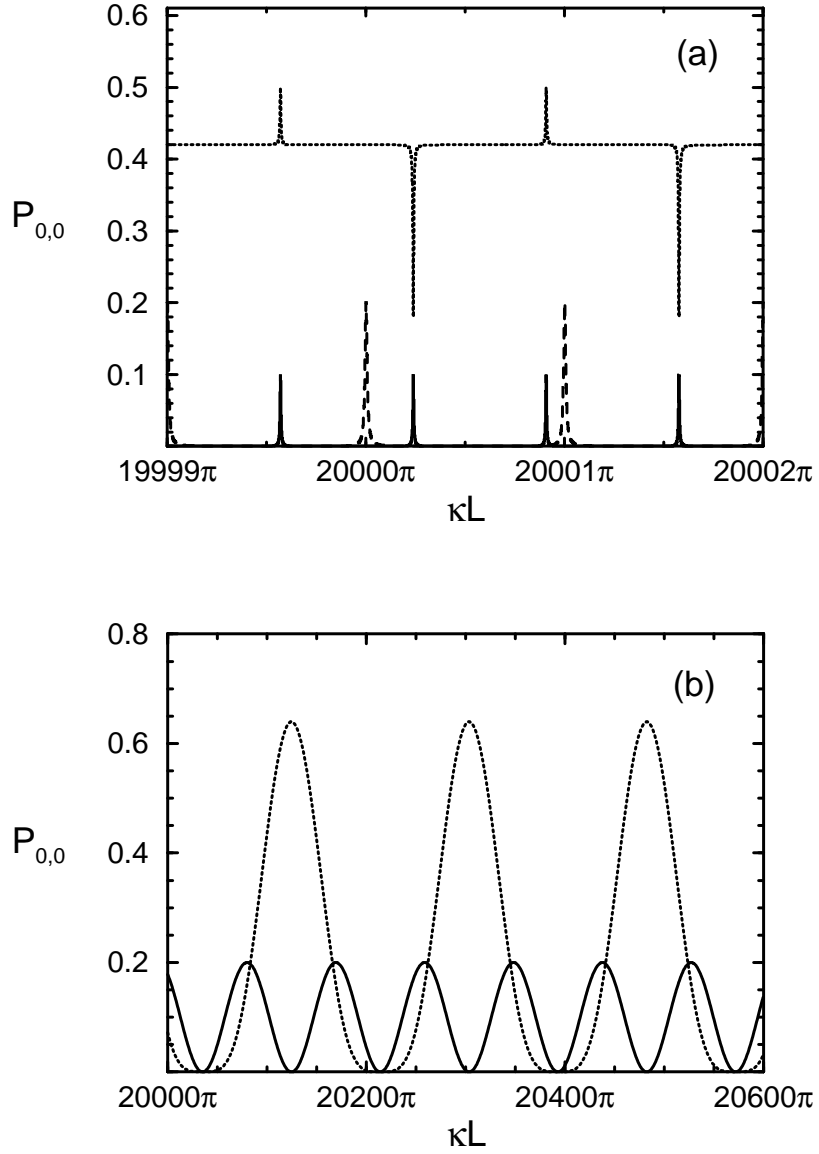


FIG. 3. The probabilities of  $a \rightarrow b_1$  (solid curve) and  $a \rightarrow b_1 \rightarrow b_2$  (dotted curve) transitions of an excited atom as a function of the length  $L$  of the cavity. The cavity is initially in vacuum state and the parameters used are  $g_2 = g_1 = 2$ ,  $k = 0.01$  [(a)],  $k = 100$  [(b)]. The dashed curve in Fig. 3(a) represents the photon emission probability of an excited two-level atom resonant with the upper transition when  $g_2 = 0$ . Actual values of the dashed curve are 2.5 times those shown. For clarity, the dotted curve in Fig. 3(a) has been displaced by 0.1 units along the Y axis.

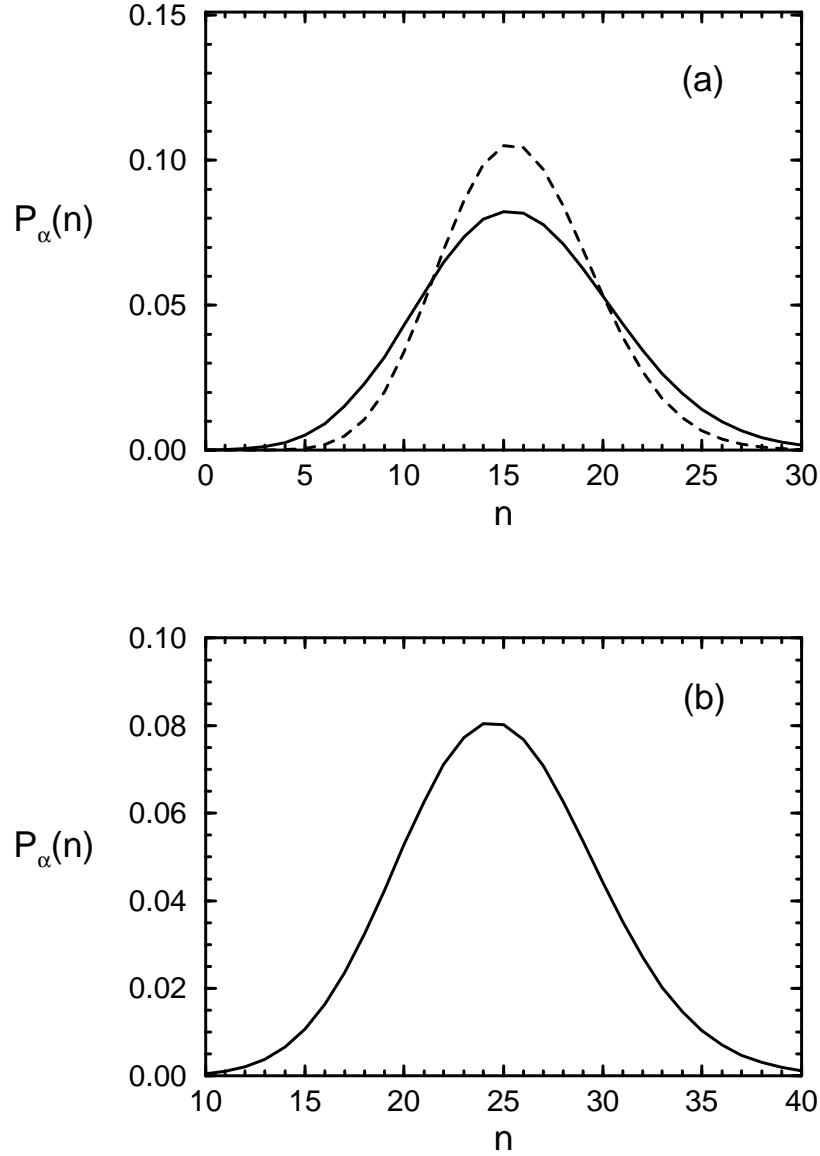


FIG. 4. The steady state distribution of photons in mode 1 (solid curve) and mode 2 (dashed curve). The parameters used are  $C_1 = C_2 = C$ ,  $n_{b1} = n_{b2} = n_b$ ,  $r=C = 50$ ,  $n_b = 0$ ,  $L = 20000$ ,  $k = 0.01$  and (a)  $g_2 = g_1 = 2$ , (b)  $g_2 = g_1 = 1$ . In the case of  $g_2 = g_1$ , the dashed curve is hardly distinguishable from the solid curve. The photon statistics for the parameter  $g_2 = g_1 = 0.5$  is approximately similar to that of  $g_2 = g_1 = 2$  except that the solid (dashed) curve corresponds to the photon distribution in mode 2 (1).

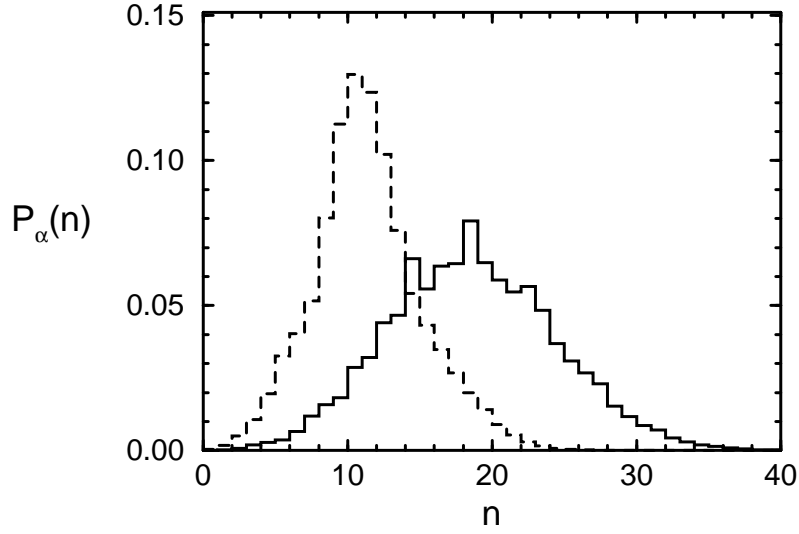


FIG .5. The steady state distribution of photons in mode 1 (solid) and mode 2 (dashed) for the same parameters of Fig. 4(a) with  $k = 100$ .

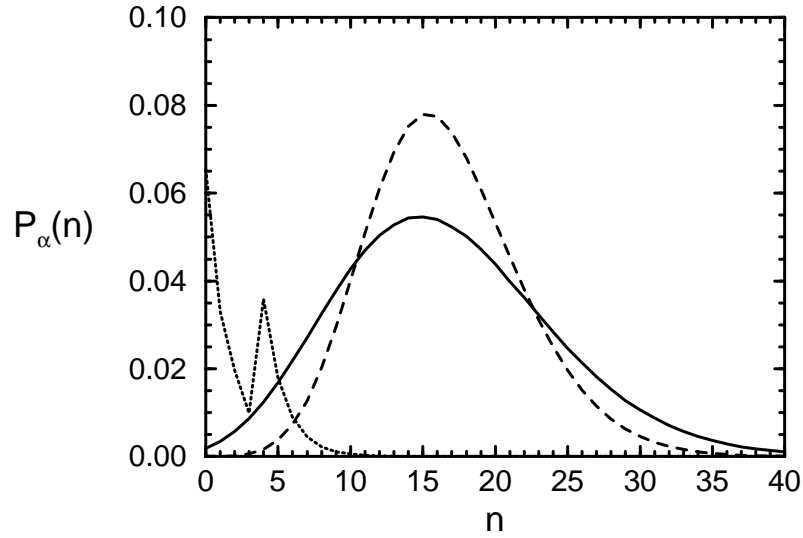


FIG .6. The steady state distribution of photons in mode 1 (solid curve) and mode 2 (dashed curve). The parameters for the calculation are  $C_1 = C_2 = C$ ,  $n_{b1} = n_{b2} = n_b$ ,  $r = C = 50$ ,  $k = 0.01$ ,  $g_2 = g_1 = 2$ ,  $L = 40000$  and  $n_b = 1$ . The dotted curve represents the photon distribution in mode 1 for the two-level problem when  $g_2 = 0$ . Actual values of the dotted curve are 5 times those shown.

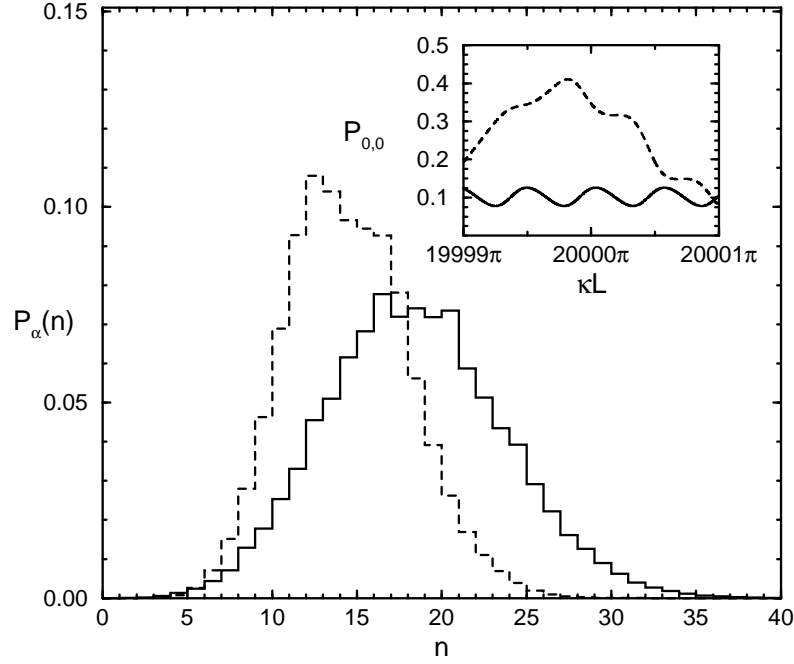


FIG .7. The steady state distribution of photons in mode 1 (solid) and mode 2 (dashed) for the same parameters of Fig. 4(a) with  $k = 1:1$ . The solid (dashed) curves in the inset represents the one-photon (two-photon) transition probabilities of an excited atom for an initial vacuum field in the cavity. The parameters used for the inset are  $g_2=g_1 = 2$  and  $k = 1:1$ :